Supplement of Atmos. Chem. Phys., 24, 4451–4472, 2024
https://doi.org/10.5194/acp-24-4451-2024-supplement

Atmospheric Chemistry and Physics
Open Access

Supplement of

Wintertime extreme warming events in the high Arctic: characteristics, drivers, trends, and the role of atmospheric rivers

Weiming Ma et al.

Correspondence to: Weiming Ma (weiming.ma@pnnl.gov) and Hailong Wang (hailong.wang@pnnl.gov)

Contents of this file:

Text S1

Figures S1 to S6

Introduction

Text S1 describes the method used in section 3.4 to decompose AR trends into a dynamical component and a thermodynamic component. Figure S1 shows the time series of the number of days per season and the number of hours per season with at least one extreme warming event defined at the grid-point scale occurred poleward of 80°N. Figure S2 shows the spatial distribution of the total number of hours with T2m >= 0℃ for all winters during 1979-2021. Figure S3 shows the climatology of surface sensible heat flux and latent heat flux during winter of 1979-2021. Figure S4 shows the temporal evolution of T2m anomalies and integrated water vapor transport (IVT) for extreme warming events. Figure S5 shows the trends in AR frequency and its dynamical and thermodynamic component. Figure S6 shows the trends in the column-integrated water vapor (IWV) and the 850 mb wind magnitude.

Text S1:

Following Ma et al. (2020), a scaling method is applied to the IVT to decompose the total AR trends into a dynamical component, which is driven by changes in the atmospheric circulation, and a thermodynamic component, which is due to changes in the moisture field. To obtain the dynamical component, the specific humidity at each grid point (3-dimential location) and time is scaled by a scaling factor $\frac{q_c}{q_m}$, where q_c and q_m are the winter climatological specific humidity and the seasonal mean specific humidity at a given season, respectively, at the same grid location to which this scaling factor applies. The scaled specific humidity is then combined with the wind field to calculate a scaled IVT. The scaled IVT along with the IVT threshold based on the original IVT are then used as input for the AR detection algorithm. This scaling method suppresses the interannual variability in the moisture field. Trends in the AR statistics based on the scaled IVT can thus be treated as the trends driven by changes in circulation, namely the dynamical trend. The difference between the total trend and the dynamical trend is then treated as the thermodynamic trend.

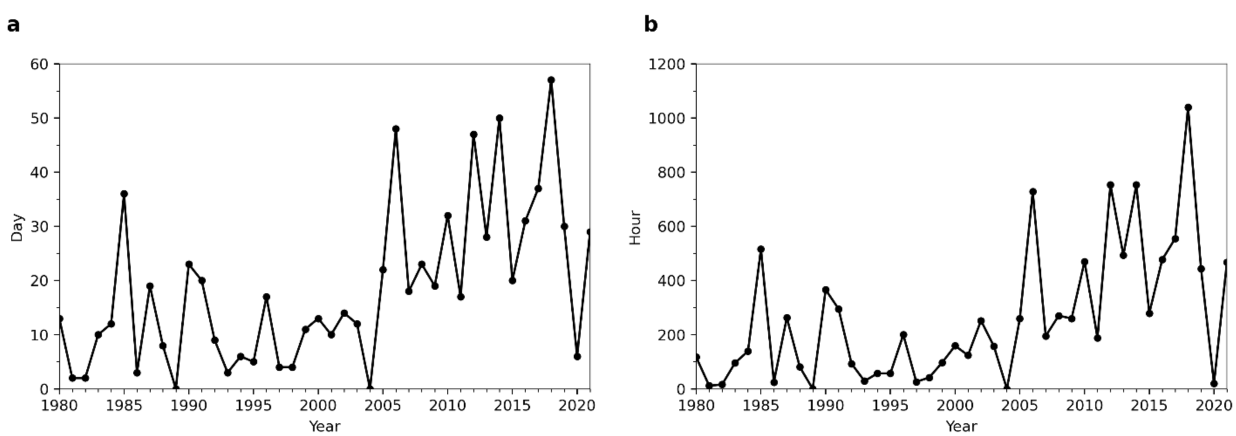

Figure S1. Time series of (a) the number of days per season and (b) the number of hours per season with at least one extreme warming event defined at the grid-point scale occurred poleward of 80°N. The trends in both time series are positive with magnitude of 6.8 days per season per decade and 114 hours per season per decade, respectively. Both trends are significant at the 0.05 level based on the Student's t-test.

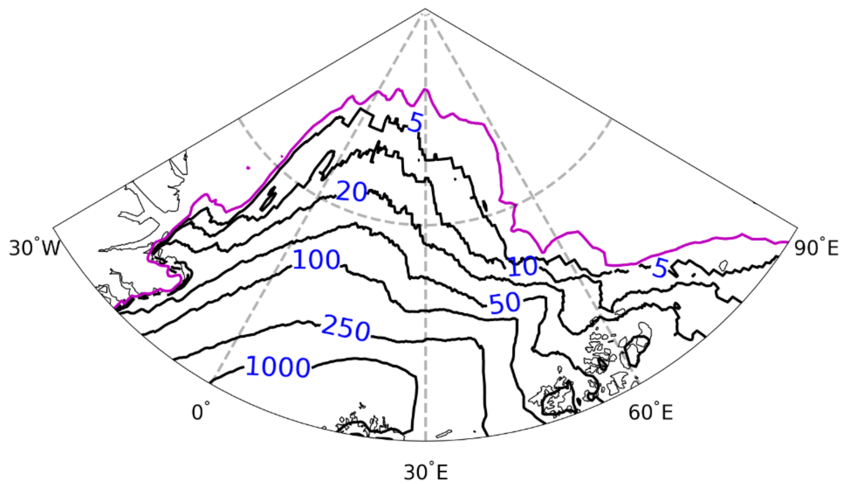

Figure S2. Spatial distribution of the total number of hours with T2m >= 0℃ for all winter during 1979-2021. The magenta contour outlines the regions that have ever experienced T2m >= 0℃.

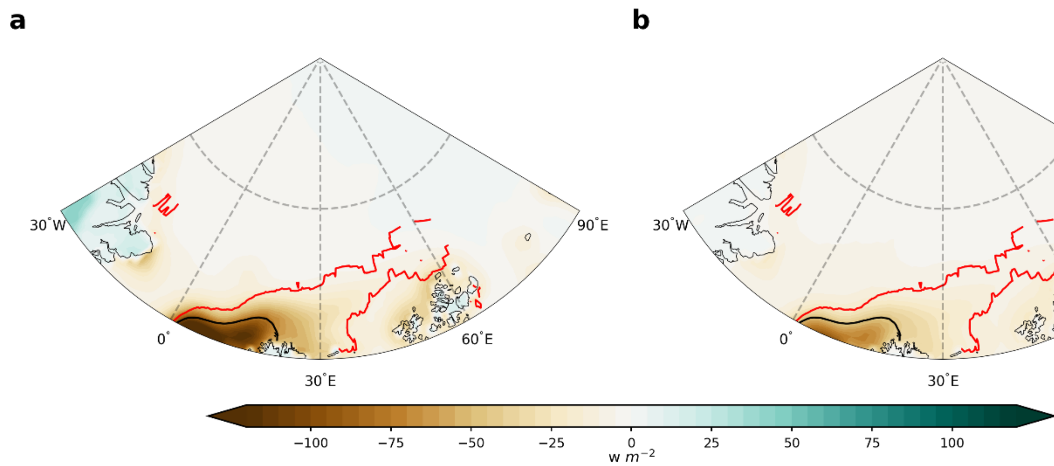

Figure S3. The climatology of (a) sensible heat flux and (b) latent heat flux during winter of 1979-2021. Overlaid are the climatological 50% sec ice concentration contour (in black) and the 50% sea ice concentration contour averaged over all extreme warming events (in red). Positive values indicate the flux is directed downward toward the surface.

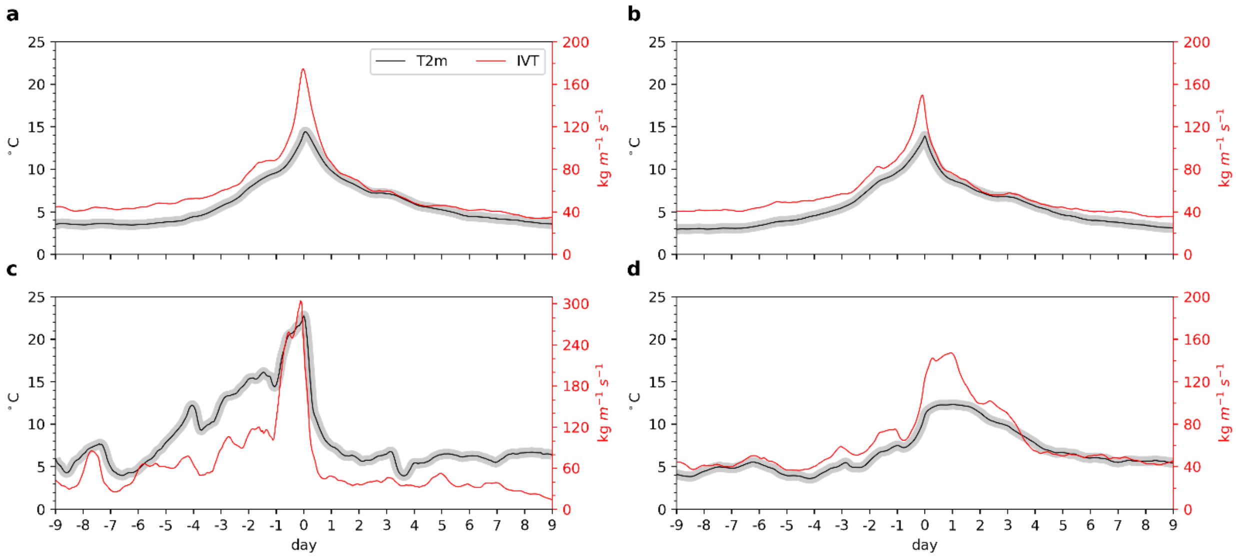

Figure S4. Temporal evolution of the T2m anomalies and IVT for (a) all the extreme warming events, (b) short duration events equatorward of 83˚N, (c) short duration events poleward of 85˚N, (d) and long duration events. The shading denotes the anomalies significant at the 0.05 level based on the Student's t-test.

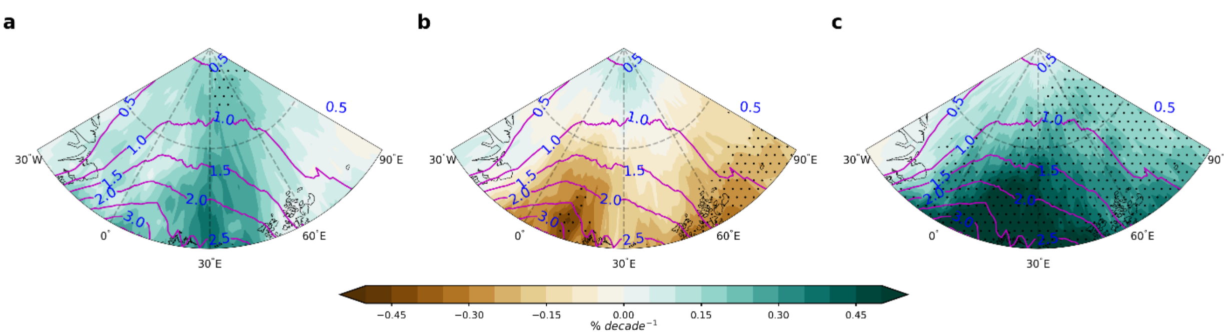

Figure S5. Spatial distribution of trends in (a) AR frequency, (b) the dynamical component and (c) the thermodynamic component. Stippled areas indicate trends significant at the 0.05 level based on the Student's t-test. The solid line contours show the climatology of the winter AR frequency (%).

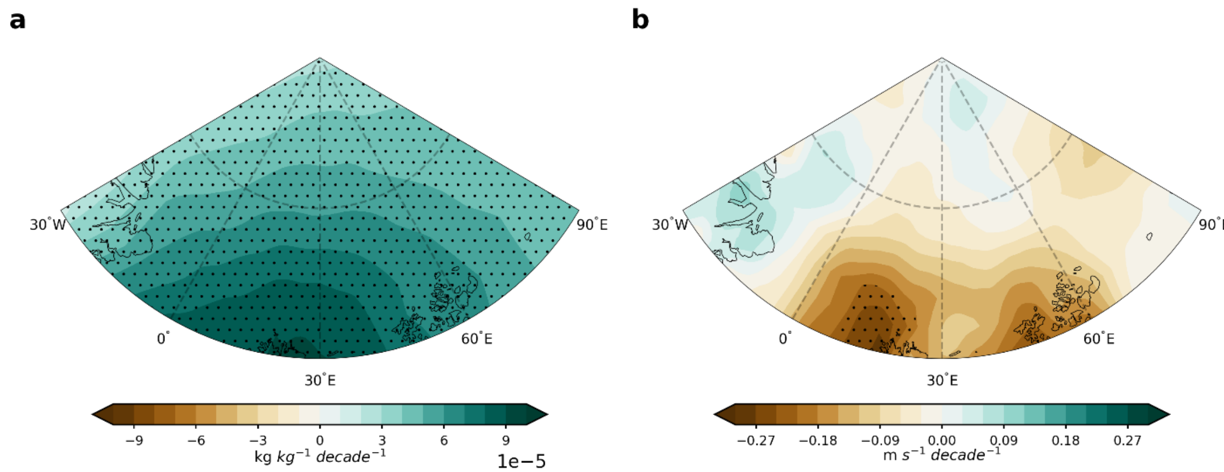

Figure S6. Spatial distribution of trends in (a) IWV and (b) 850 mb wind speed. Stippled areas indicate trends significant at the 0.05 level based on the Student's t-test.

Reference:

Ma, W., Chen, G., and Guan, B.: Poleward Shift of Atmospheric Rivers in the Southern Hemisphere in Recent Decades, Geophys. Res. Lett., 47, 1–11, https://doi.org/10.1029/2020GL089934, 2020.